Spectral folding and two-channel filter-banks on arbitrary graphs

Eduardo Pavez, Benjamin Girault, Antonio Ortega, Philip A Chou

SPECTRAL FOLDING AND TWO-CHANNEL FILTER-BANKS ON ARBITRARY GRAPHS

Eduardo Pavez[⋆], *Benjamin Girault*[#⋆], *Antonio Ortega*[⋆], *Philip A. Chou*[†]

[⋆]University of Southern California, Los Angeles, California, USA
[#] Université de Rennes, ENSAI, CNRS, CREST-UMR 9194, Rennes, FRANCE
[†]Google Research, Seattle, Washington, USA

ABSTRACT

In the past decade, several multi-resolution representation theories for graph signals have been proposed. Bipartite filter-banks stand out as the most natural extension of time domain filter-banks, in part because perfect reconstruction, orthogonality and bi-orthogonality conditions in the graph spectral domain resemble those for traditional filter-banks. Therefore, many of the well known orthogonal and bi-orthogonal designs can be easily adapted for graph signals. A major limitation is that this framework can only be applied to the normalized Laplacian of bipartite graphs. In this paper we extend this theory to arbitrary graphs and positive semi-definite variation operators. Our approach is based on a different definition of the graph Fourier transform (GFT), where orthogonality is defined with respect to the $\mathbf{Q}$ inner product. We construct GFTs satisfying a spectral folding property, which allows us to easily construct orthogonal and bi-orthogonal perfect reconstruction filter-banks. We illustrate signal representation and computational efficiency of our filter-banks on 3D point clouds with hundreds of thousands of points.

Index Terms— graph filterbank, graph Fourier transform, multiresolution representation, two channel filterbank

1. INTRODUCTION

Graph signal processing (GSP) provides a toolbox for analysis and manipulation of signals living in irregular domains [1, 2]. Given the success of multi-resolution representations (MRR) to analyze and process traditional signals [3], significant efforts have been put into extending MRRs for graph signals [4].

Applications often require these MRRs to: (i) be perfect reconstruction (invertible), (ii) be critically sampled (non redundant), (iii) be orthogonal, and (iv) have compact support (polynomial filter implementation). In the graph setting, it has proven challenging to find theories that satisfy more than a few of these properties simultaneously. Current theories require strong assumptions on the graph topology (e.g., bipartite [5, 6], circulant [7]), and are valid for a single type of graph operator (e.g., normalized Laplacian or adjacency). Narang and Ortega [5, 6] proposed two channel filter-banks on bipartite graphs, composed of graph filters, vertex down-sampling, and vertex up-sampling operators (see Figure 1). These bipartite filter-banks (BFB) obey (i), (ii), and either (iii) or (iv), can be designed in the frequency domain, and can be implemented using low degree polynomials. In addition, regular domain filter-banks can be easily converted to the graph domain [5, 6, 8, 9, 10]. Given their strong theoretical properties and efficient implementations, BFB have found numerous applications [11, 12, 13, 14].

Author's email: pavezcar@usc.edu. This work was funded in part by a Google Faculty Research Award.

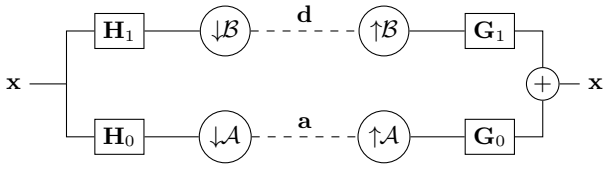

Fig. 1: Perfect reconstruction two channel filter-bank with analysis filters $\mathbf{H}_0$, $\mathbf{H}_1$, and synthesis filters $\mathbf{G}_0$ and $\mathbf{G}_1$. $\mathbf{a}$ and $\mathbf{d}$ denote approximation (low pass) and detail (high pass) coefficients respectively. Sampling sets are denoted by $\mathcal{A}$ and $\mathcal{B}$.

Despite all these remarkable properties, BFB theory [5, 6] only applies to normalized Laplacians and adjacency matrices of bipartite graphs. These are major limitations since the graph structure is rarely bipartite (which dictates the down-sampling operator), whereas the graph variation operator (or graph shift) is determined by the application. To overcome these issues, we propose a new theory that can be applied to: 1) arbitrary graphs, 2) any vertex partition for down-sampling, and 3) positive semi-definite variation operators (see [15, 16, 17, 18] for examples). The proposed filter-banks also satisfy (i), (ii), and either (iii) or (iv), as with BFBs.

We consider the $(\mathbf{M}, \mathbf{Q})$ graph Fourier transform ($(\mathbf{M}, \mathbf{Q})$-GFT), a generalization of the GFT to arbitrary finite dimensional Hilbert spaces [15, 19] with inner product $\langle \mathbf{x}, \mathbf{y} \rangle_{\mathbf{Q}} = \mathbf{y}^\top \mathbf{Q} \mathbf{x}$ and variation operator $\mathbf{M}$. BFB theory is built upon a *spectral folding* property of the eigenvectors and eigenvalues of the normalized Laplacian of bipartite graphs [20]. We follow a similar strategy and prove a new *spectral folding* property for the $(\mathbf{M}, \mathbf{Q})$-GFT. Interestingly, our perfect reconstruction and orthogonality conditions match those of the BFB framework [5, 6], and as a result their filter designs, or any of the more recent improvements [8, 9] can be reused. When the graph is bipartite, and $\mathbf{M}$ is the normalized or combinatorial Laplacian, we recover the nonZeroDC and ZeroDC filter-banks, respectively [5, 6].

Early MRRs on arbitrary graphs were constructed by scaling and shifting spectral graph filters [21, 22, 23]. These methods are difficult to invert (e.g., requiring least squares), are not critically sampled, and lack orthogonality. More recent approaches are redundant [24, 25], lack perfect reconstruction [26, 27], or change the graph to a bipartite one [28, 29, 30, 5]. While some of these approaches [28, 29, 5] can exploit efficient filter-bank implementations, once a sparse bipartite graph is available, obtaining the bipartite graph itself, either by graph approximation or through graph learning may be computationally infeasible for large graphs. More recently, [31] proposed graph filter-banks with spectral domain down-sampling. This sampling operator induces spectral folding of the GFT which is exploited to obtain perfect reconstruction conditions. Although this approach can be used for arbitrary graphs and variation operators, it

requires computing a full GFT, which does not scale to large graphs.

We show in our experiments with 3D point clouds, that in contrast to previous approaches, the proposed filter-banks can be implemented efficiently on large graphs (e.g., with hundreds of thousands of nodes), as long as these are sparse, and outperform BFBs in energy compaction and run time. The rest of the paper is organized as follows. In Sections 2 and 3 we review the fundamentals of GSP on arbitrary Hilbert spaces, and two channel filter-banks on bipartite graphs, respectively. Our theory is presented in Section 4. We end this paper with numerical results and conclusions in Sections 5 and 6, respectively.

2. GSP IN ARBITRARY HILBERT SPACES

Scalars, vectors and matrices are written in lower case regular, lower case bold and upper case bold respectively (e.g., a, $\mathbf{b}$, $\mathbf{C}$). Positive definite and semi-definite matrices are denoted by $\mathbf{A} \succ 0$ and $\mathbf{A} \succeq 0$ respectively. Consider a weighted undirected graph $\mathcal{G} = (\mathcal{V}, \mathcal{E}, \mathbf{M})$ with vertex set $\mathcal{V} = \{1, 2, \cdots, n\}$, edge set $\mathcal{E} \subset \mathcal{V} \times \mathcal{V}$, and variation operator $\mathbf{M} = (m_{ij})$, satisfying $m_{ij} = m_{ji} \neq 0$ when $ij \in \mathcal{E}$, and $m_{ij} = 0$ otherwise. A graph signal is a function $x : \mathcal{V} \to \mathbb{R}$, that can be represented by a vector $\mathbf{x} = [x_1, \cdots, x_n]^\top$. The variation operator is assumed to be positive semi-definite, and the variation of a signal is $\Delta(\mathbf{x}) = \mathbf{x}^\top \mathbf{M} \mathbf{x} \geq 0$. Intuitively, signals with increased variation are said to have higher frequency content. We will further assume that $\mathbf{M}$ is irregular, that is, the graph is connected. Typical examples of variation operators include the combinatorial and normalized Laplacian matrices. For a symmetric non negative matrix $\mathbf{W} = (w_{ij})$, degree of node i is $d_i = \sum_{j \in \mathcal{V}} w_{ij}$, and the degree matrix is $\mathbf{D} = \operatorname{diag}(d_1, \cdots, d_n)$. The combinatorial Laplacian is $\mathbf{L} = \mathbf{D} - \mathbf{W}$, while the normalized Laplacian is $\boldsymbol{\mathcal{L}} = \mathbf{D}^{-1/2}\mathbf{L}\mathbf{D}^{-1/2} = \mathbf{I} - \mathbf{D}^{-1/2}\mathbf{W}\mathbf{D}^{-1/2}$. [15] introduced the idea of using an inner product $\langle \mathbf{x}, \mathbf{y} \rangle_{\mathbf{Q}} = \mathbf{y}^\top \mathbf{Q} \mathbf{x}$, and induced norm given by $\|\mathbf{x}\|_{\mathbf{Q}} = \sqrt{\langle \mathbf{x}, \mathbf{x} \rangle_{\mathbf{Q}}}$, with $\mathbf{Q} \succ 0$. The $(\mathbf{M}, \mathbf{Q})$-GFT basis vectors are the columns of $\mathbf{U} = [\mathbf{u}_1, \cdots, \mathbf{u}_n]$, which solve the generalized eigenvalue problem

$$\mathbf{M}\mathbf{u}_k = \lambda_k \mathbf{Q}\mathbf{u}_k, \tag{1}$$

and $0 \leq \lambda_1 \leq, \cdots, \leq \lambda_n$. The set of eigenvalues (spectrum) of a graph is denoted by $\sigma(\mathbf{M}, \mathbf{Q})$. The generalized eigenvectors are $\mathbf{Q}$-orthonormal, hence $\|\mathbf{u}_i\|_{\mathbf{Q}} = 1, \quad \forall i \in \mathcal{V}$, and $\langle \mathbf{u}_i, \mathbf{u}_j \rangle_{\mathbf{Q}} = 0, \quad \forall i \neq j$, that is, $\mathbf{U}^\top \mathbf{Q} \mathbf{U} = \mathbf{I}$ in matrix form. A graph signal $\mathbf{x}$ has the following repesentation in the $(\mathbf{M}, \mathbf{Q})$-GFT basis

$$\mathbf{x} = \sum_{i=1}^{n} \langle \mathbf{x}, \mathbf{u}_i \rangle_{\mathbf{Q}} \mathbf{u}_i = \mathbf{U}\hat{\mathbf{x}}. \tag{2}$$

The $(\mathbf{M}, \mathbf{Q})$-GFT of $\mathbf{x}$ is denoted by $\hat{\mathbf{x}}$, with coordinates $\hat{x}_i = \langle \mathbf{x}, \mathbf{u}_i \rangle_{\mathbf{Q}}$. In matrix form this corresponds to $\hat{\mathbf{x}} = \mathbf{U}^\top \mathbf{Q} \mathbf{x}$, while the inverse transform is given by $\mathbf{x} = \mathbf{U}\hat{\mathbf{x}}$, since $\mathbf{U}\mathbf{U}^\top \mathbf{Q} = \mathbf{I}$. A linear operator $\mathbf{H}$ is a spectral filter if there is a function $h : \mathbb{R}_+ \to \mathbb{R}$ so that $\mathbf{H} = \mathbf{U} h(\mathbf{\Lambda}) \mathbf{U}^\top \mathbf{Q} = h(\mathbf{Z})$, where $\mathbf{Z} = \mathbf{Q}^{-1}\mathbf{M} = \mathbf{U}\mathbf{\Lambda}\mathbf{U}^\top \mathbf{Q}$ is the fundamental matrix, and $\mathbf{\Lambda} = \operatorname{diag}(\lambda_1, \cdots, \lambda_n)$.

3. TWO CHANNEL FILTER-BANKS

In this section we define two channel filter-banks on arbitrary graphs, and review the BFB theory [5, 6]. A two channel filter-bank is depicted in Figure 1. The analysis filters are $\mathbf{H}_0$ and $\mathbf{H}_1$, while the synthesis filters correspond to $\mathbf{G}_0$ and $\mathbf{G}_1$. Consider the set $\mathcal{A}$ and $\mathcal{B} = \mathcal{A} \setminus \mathcal{V}$, which form a partition of the vertex set $\mathcal{V}$. Without loss of generality we assume that $\mathcal{A} = \{1, 2, \cdots, |\mathcal{A}|\}$. Down-sampling a signal $\mathbf{x}$ on a set $\mathcal{A}$ corresponds to keeping the entries $x_i : i \in \mathcal{A}$, and discarding the rest. This can be represented by $\mathbf{x}_{\mathcal{A}} = \mathbf{S}_{\mathcal{A}}\mathbf{x}$, where $\mathbf{S}_{\mathcal{A}} = [\mathbf{I}_{\mathcal{A}}, \mathbf{0}]$ is a $|\mathcal{A}| \times |\mathcal{V}|$ selection matrix. The up-sampling operator is $\mathbf{S}_{\mathcal{A}}^\top$. Down-sampling followed by up-sampling sets to zero the entries in $\mathcal{B}$, thus $\mathbf{S}_{\mathcal{A}}^\top \mathbf{x}_{\mathcal{A}} = \mathbf{S}_{\mathcal{A}}^\top \mathbf{S}_{\mathcal{A}} \mathbf{x} = \begin{bmatrix} \mathbf{x}_{\mathcal{A}}^\top & \mathbf{0} \end{bmatrix}^\top$.

3.1. Vertex domain conditions for arbitrary graphs

The analysis operator (filtering and down-sampling) from Fig. 1 is

$$\mathbf{T}_a = \mathbf{S}_{\mathcal{A}}^\top \mathbf{S}_{\mathcal{A}} \mathbf{H}_0 + \mathbf{S}_{\mathcal{B}}^\top \mathbf{S}_{\mathcal{B}} \mathbf{H}_1 = \begin{bmatrix} \mathbf{S}_{\mathcal{A}} \mathbf{H}_0 \\ \mathbf{S}_{\mathcal{B}} \mathbf{H}_1 \end{bmatrix}. \tag{3}$$

The outputs of the low pass and high pass channels, called approximation $\mathbf{a}$ and detail $\mathbf{d}$ coefficients, respectively, are given by:

$$\mathbf{T}_a \mathbf{x} = \begin{bmatrix} \mathbf{a} \\ \mathbf{d} \end{bmatrix} = \begin{bmatrix} \mathbf{S}_{\mathcal{A}} \mathbf{H}_0 \mathbf{x} \\ \mathbf{S}_{\mathcal{B}} \mathbf{H}_1 \mathbf{x} \end{bmatrix}. \tag{4}$$

The synthesis operator has a similar expression

$$\mathbf{T}_s = \mathbf{G}_0 \mathbf{S}_{\mathcal{A}}^\top \mathbf{S}_{\mathcal{A}} + \mathbf{G}_1 \mathbf{S}_{\mathcal{B}}^\top \mathbf{S}_{\mathcal{B}} = \begin{bmatrix} \mathbf{G}_0 \mathbf{S}_{\mathcal{A}}^\top & \mathbf{G}_1 \mathbf{S}_{\mathcal{B}}^\top \end{bmatrix}. \tag{5}$$

We say that a two channel filter-bank is **perfect reconstruction (PR)** if $\mathbf{T}_s \mathbf{T}_a = \mathbf{T}_a \mathbf{T}_s = \mathbf{I}$. A linear operator $\mathbf{T}$ is **$\mathbf{Q}$-orthogonal** if for each $\mathbf{x}$, the norm of the transformed signal is preserved, that is, $\|\mathbf{T}\mathbf{x}\|_{\mathbf{Q}} = \|\mathbf{x}\|_{\mathbf{Q}}$. In matrix form this corresponds to $\mathbf{T}^\top \mathbf{Q} \mathbf{T} = \mathbf{Q}$. For a PR two channel filter-bank, $\mathbf{T}_a$ is $\mathbf{Q}$-orthogonal if and only if $\mathbf{T}_s$ is $\mathbf{Q}$-orthogonal. Finding operators $\mathbf{T}_a$, $\mathbf{T}_s$ that are orthogonal and PR is not that difficult, in fact, any non-singular orthogonal matrix can be used for $\mathbf{T}_a$, and the synthesis operator can be chosen as $\mathbf{T}_s = \mathbf{Q}^{-1} \mathbf{T}_a^\top \mathbf{Q}$. The challenge is finding operators that exploit the graph structure, and that can be efficiently implemented on large arbitrary graphs. In the next subsection we review the approach of [5, 6] to design BFB using spectral graph filters.

3.2. Spectral domain conditions for bipartite graphs

BFBs can be constructed on bipartite graphs:

Definition 1. A graph $\mathcal{G} = (\mathcal{V}, \mathcal{E})$ is bipartite on $(\mathcal{A}, \mathcal{B})$, if i) $(\mathcal{A}, \mathcal{B})$ forms a partition, that is, $\mathcal{A} \cap \mathcal{B} = \emptyset$, and $\mathcal{A} \cup \mathcal{B} = \mathcal{V}$, and ii) for all $(i, j) \in \mathcal{E}$, $i \in \mathcal{A}$ and $j \in \mathcal{B}$, or $i \in \mathcal{B}$ and $j \in \mathcal{A}$.

In bipartite graphs, only edges between sets $\mathcal{A}$ and $\mathcal{B}$ are allowed, therefore the Laplacian matrices have the form

$$\mathbf{L} = \begin{bmatrix} \mathbf{D}_{\mathcal{A}} & -\mathbf{W}_{\mathcal{A}\mathcal{B}} \\ -\mathbf{W}_{\mathcal{B}\mathcal{A}} & \mathbf{D}_{\mathcal{B}} \end{bmatrix}, \quad \boldsymbol{\mathcal{L}} = \begin{bmatrix} \mathbf{I}_{\mathcal{A}} & -\tilde{\mathbf{W}}_{\mathcal{A}\mathcal{B}} \\ -\tilde{\mathbf{W}}_{\mathcal{B}\mathcal{A}} & \mathbf{I}_{\mathcal{B}} \end{bmatrix}, \tag{6}$$

where $\boldsymbol{\mathcal{L}} = \mathbf{D}^{-1/2}\mathbf{L}\mathbf{D}^{-1/2} = \mathbf{I} - \tilde{\mathbf{W}}$, and $\tilde{\mathbf{W}} = \mathbf{D}^{-1/2}\mathbf{W}\mathbf{D}^{-1/2}$. Spectral filters are defined using the $(\boldsymbol{\mathcal{L}}, \mathbf{I})$-GFT, thus $\mathbf{Z} = \boldsymbol{\mathcal{L}}$, and

$$\mathbf{H}_i = h_i(\boldsymbol{\mathcal{L}}), \quad \mathbf{G}_i = g_i(\boldsymbol{\mathcal{L}}), \quad \text{for } i \in \{0, 1\}. \tag{7}$$

We define $\mathbf{J} = \operatorname{diag}(\mathbf{f})$, where $\mathbf{f}_i = 1$ if $i \in \mathcal{A}$, and $\mathbf{f}_i = -1$ when $i \in \mathcal{B}$. Then $\mathbf{S}_{\mathcal{A}}^\top \mathbf{S}_{\mathcal{A}} = \frac{1}{2}(\mathbf{I} + \mathbf{J})$, and $\mathbf{S}_{\mathcal{B}}^\top \mathbf{S}_{\mathcal{B}} = \frac{1}{2}(\mathbf{I} - \mathbf{J})$, and the PR condition becomes

$$\mathbf{I} = \frac{1}{2}\left(\mathbf{G}_0\mathbf{H}_0 + \mathbf{G}_1\mathbf{H}_1\right) + \frac{1}{2}\left(\mathbf{G}_0\mathbf{J}\mathbf{H}_0 - \mathbf{G}_1\mathbf{J}\mathbf{H}_1\right). \tag{8}$$

The BFB framework achieves PR by designing filters that obey

$$\mathbf{G}_0\mathbf{H}_0 + \mathbf{G}_1\mathbf{H}_1 = 2\mathbf{I}, \quad \text{and} \quad \mathbf{G}_0\mathbf{J}\mathbf{H}_0 - \mathbf{G}_1\mathbf{J}\mathbf{H}_1 = \mathbf{0}. \tag{9}$$

Theorem 1. *[5] For a BFB with filters given by (7), a necessary and sufficient condition for PR is that* $\forall \lambda \in \sigma(\boldsymbol{\mathcal{L}}, \mathbf{I})$,

$$h_0(\lambda)g_0(\lambda) + h_1(\lambda)g_1(\lambda) = 2 \tag{10}$$
$$h_0(\lambda)g_0(2-\lambda) - h_1(\lambda)g_1(2-\lambda) = 0. \tag{11}$$

$\mathbf{I}$-orthogonal filter-banks can be realized if and only if for all $\lambda \in \sigma(\boldsymbol{\mathcal{L}}, \mathbf{I})$, the filters also satisfy

$$h_0^2(\lambda) + h_1^2(\lambda) = 2, \tag{12}$$
$$h_0(\lambda)h_0(2-\lambda) - h_1(\lambda)h_1(2-\lambda) = 0. \tag{13}$$

Orthogonal filter-banks are PR, while the converse is not true in general. In fact, filters h_0, h_1, g_0, g_1 obey (12) and (13), if and only if, they obey (10), (11) and $h_i = g_i$. These filters are not polynomial, thus requiring full eigendecomposition for implementation. To overcome this, filters can be approximated with Chebyshev polynomials [23, 8]. An alternative is to use PR bi-orthogonal filters

$$h_0(\lambda) = g_1(2-\lambda), \quad h_1(\lambda) = g_0(2-\lambda), \tag{14}$$

which can be designed to be near orthogonal and polynomial [6]. The proofs of orthogonality and PR (Theorem 1) use Proposition 1, which holds only for the normalized Laplacian of bipartite graphs.

Proposition 1. *[20][Spectral folding.] If* $\boldsymbol{\mathcal{L}}\mathbf{u} = \lambda\mathbf{u}$, *then* $\mathbf{J}\mathbf{u}$ *is an eigenvector with eigenvalue* $2-\lambda$.

To the best of our knowledge no other variation operators have this property for bipartite or arbitrary graphs.

4. MAIN RESULTS

We start by establishing conditions under which the $(\mathbf{M}, \mathbf{Q})$-GFT has the spectral folding property.

Theorem 2 (Spectral folding)**.** *Consider an arbitrary partition of the vertices,* $\mathcal{A}$ *and* $\mathcal{B} = \mathcal{V} \setminus \mathcal{A}$. *Without loss of generality we assume* $\mathcal{A} = \{1, 2, \cdots, |\mathcal{A}|\}$. *Let* $\mathbf{Q} \succ 0$ *and the variation operator be*

$$\mathbf{M} = \begin{bmatrix} \mathbf{M}_{\mathcal{A}\mathcal{A}} & \mathbf{M}_{\mathcal{A}\mathcal{B}} \\ \mathbf{M}_{\mathcal{B}\mathcal{A}} & \mathbf{M}_{\mathcal{B}\mathcal{B}} \end{bmatrix} \succeq 0, \tag{15}$$

then the following statements are equivalent:

1. *The inner product matrix is equal to*

$$\mathbf{Q} = \begin{bmatrix} \mathbf{M}_{\mathcal{A}\mathcal{A}} & \mathbf{0} \\ \mathbf{0} & \mathbf{M}_{\mathcal{B}\mathcal{B}} \end{bmatrix}. \tag{16}$$

2. *There is a full set of generalized eigenvectors, and*

$$\mathbf{M}\mathbf{u} = \lambda\mathbf{Q}\mathbf{u} \iff \mathbf{M}\mathbf{J}\mathbf{u} = (2-\lambda)\mathbf{Q}\mathbf{J}\mathbf{u}. \tag{17}$$

Due to space limitations, we only sketch the proof of 1) $\Rightarrow$ 2). A complete proof can be found in [32]. Let $\mathbf{u} = [\mathbf{u}_{\mathcal{A}}^\top, \mathbf{u}_{\mathcal{B}}^\top]^\top$ be a generalized eigenvector of $\mathbf{M}$ with eigenvalue λ, then

$$\mathbf{M}_{\mathcal{A}\mathcal{A}}\mathbf{u}_{\mathcal{A}} + \mathbf{M}_{\mathcal{A}\mathcal{B}}\mathbf{u}_{\mathcal{B}} = \lambda\mathbf{Q}_{\mathcal{A}}\mathbf{u}_{\mathcal{A}}, \ \mathbf{M}_{\mathcal{B}\mathcal{A}}\mathbf{u}_{\mathcal{A}} + \mathbf{M}_{\mathcal{B}\mathcal{B}}\mathbf{u}_{\mathcal{B}} = \lambda\mathbf{Q}_{\mathcal{B}}\mathbf{u}_{\mathcal{B}}.$$

Set $\mathbf{v} = \mathbf{J}\mathbf{u} = [\mathbf{u}_{\mathcal{A}}^\top, -\mathbf{u}_{\mathcal{B}}^\top]^\top$, and compute $\mathbf{M}\mathbf{v}$. Using the fact that $\mathbf{u}$ is a generalized eigenvector, and (16) produces the desired result. For this $(\mathbf{M}, \mathbf{Q})$-GFT, the fundamental matrix is:

$$\mathbf{Z} = \mathbf{Q}^{-1}\mathbf{M} = \begin{bmatrix} \mathbf{I}_{\mathcal{A}} & \mathbf{M}_{\mathcal{A}\mathcal{A}}^{-1}\mathbf{M}_{\mathcal{A}\mathcal{B}} \\ \mathbf{M}_{\mathcal{B}\mathcal{B}}^{-1}\mathbf{M}_{\mathcal{B}\mathcal{A}} & \mathbf{I}_{\mathcal{B}} \end{bmatrix} = \mathbf{U}\boldsymbol{\Lambda}\mathbf{U}^\top\mathbf{Q},$$

and $\boldsymbol{\Lambda} = \mathrm{diag}(\lambda_1, \lambda_2, \cdots, \lambda_n)$. This $(\mathbf{M}, \mathbf{Q})$-GFT shares some properties with the $(\boldsymbol{\mathcal{L}}, \mathbf{I})$-GFT of bipartite graphs. First, the generalized eigenvalues obey $0 \leq \lambda_i \leq 2$, and inequalities become strict when $\mathbf{M}$ is non-singular. Second, the eigenvalue $\lambda = 1$ has multiplicity at least $||\mathcal{A}| - |\mathcal{B}||$, thus the middle graph frequency is less selective when the down-sampling sets have uneven size. Finally, when $\mathbf{M} = \mathbf{L} + \mathbf{V}$ and $\mathbf{V}$ is diagonal, i.e., $\mathbf{L}$ is a generalized Laplacian [17], the multiplicity of λ_1 (smallest eigenvalue) is equal to the number of connected components of the graph. Now we state our result for PR filter-banks.

Theorem 3 (Perfect reconstruction)**.** *For any positive semi definite variation operator* $\mathbf{M}$, *and any vertex partition* $\mathcal{V} = \mathcal{A} \cup \mathcal{B}$. *Choose the inner product matrix* $\mathbf{Q}$ *according to Theorem 2, and spectral graph filters for* $i \in \{0, 1\}$

$$\mathbf{H}_i = \mathbf{U}h_i(\boldsymbol{\Lambda})\mathbf{U}^\top\mathbf{Q}, \quad \mathbf{G}_i = \mathbf{U}g_i(\boldsymbol{\Lambda})\mathbf{U}^\top\mathbf{Q}. \tag{18}$$

The functions h_i, g_i *for* $i \in \{0, 1\}$ *obey conditions (10) and (11) for all* $\lambda \in \sigma(\mathbf{M}, \mathbf{Q})$, *if and only if the filter-bank of Figure 1 is PR.*

The proof follows from Theorem 2 and similar arguments as those used in [5] to prove (9). Theorem 3 implies that our framework can be implemented using filters designed for bipartite graphs (see [5, 6, 9, 8]). We can also construct $\mathbf{Q}$-orthogonal filter-banks.

Theorem 4 (Parseval)**.** *Under the conditions of Theorem 3, the analysis filters obey (12) and (13) for all* $\lambda \in \sigma(\mathbf{M}, \mathbf{Q})$, *if and only if,*

$$\langle \mathbf{T}_a\mathbf{x}, \mathbf{T}_a\mathbf{y} \rangle_{\mathbf{Q}} = \langle \mathbf{x}, \mathbf{y} \rangle_{\mathbf{Q}}.$$

Theorem 4 could be stated replacing $\mathbf{T}_a$ by $\mathbf{T}_s$. We have preservation of the $\mathbf{Q}$ norm, thus $\|\mathbf{T}_a\mathbf{x}\|_{\mathbf{Q}}^2 = \|\mathbf{x}\|_{\mathbf{Q}}^2$, and $\|\mathbf{T}_s\mathbf{x}\|_{\mathbf{Q}}^2 = \|\mathbf{x}\|_{\mathbf{Q}}^2$. When $\mathbf{Q} = \mathbf{I}$, the synthesis operator is the transpose of $\mathbf{T}_a$, however, in general we have the relation $\mathbf{T}_s = \mathbf{Q}^{-1}\mathbf{T}_a^\top\mathbf{Q}$. The authors in [6] showed that orthogonal filter-banks cannot be implemented with polynomials of $\boldsymbol{\mathcal{L}}$. The same arguments lead to $\mathbf{Q}$-orthogonal filter-banks not having implementations with polynomial of $\mathbf{Z}$. As an alternative, bi-orthogonal filters (14) were proposed, which have polynomials implementations, and can be designed to be approximately $\mathbf{Q}$-orthogonal (see [Section III-B][6]), and satisfy

$$\alpha\|\mathbf{x}\|_{\mathbf{Q}} \lesssim \|\mathbf{T}_*\mathbf{x}\|_{\mathbf{Q}} \lesssim \beta\|\mathbf{x}\|_{\mathbf{Q}} \ \ \forall \mathbf{x}, \tag{19}$$

where $*$ can be a or s, and

$$\alpha^2 = \frac{1}{2}\inf_{\lambda\in[0,2]}(h_0^2(\lambda) + h_1^2(\lambda)), \ \beta^2 = \frac{1}{2}\sup_{\lambda\in[0,2]}(h_0^2(\lambda) + h_1^2(\lambda)).$$

Remark 1. *The zeroDC filter-banks [6], were introduced so that the smoothest basis function is constant. This approach can be implemented by multiplying the input by* $\mathbf{D}^{1/2}$ *before applying the analysis filter-bank, and multiplying by* $\mathbf{D}^{-1/2}$ *at the output of the synthesis filter-bank. This ensures that a constant input signal has zero response in the high pass channel. Bi-orthogonal zero-DC filter-banks can be implemented with polynomials of the random walk Laplacian of a bipartite graph [6]. The zeroDC filter-banks can be derived as a special case of our framework, since for bipartite graphs with Laplacian* $\mathbf{L}$, *the inner product matrix from Proposition 2 is* $\mathbf{Q} = \mathbf{D}$, *and the fundamental matrix is the random walk Laplacian* $\mathbf{Z} = \mathbf{D}^{-1}\mathbf{L}$.

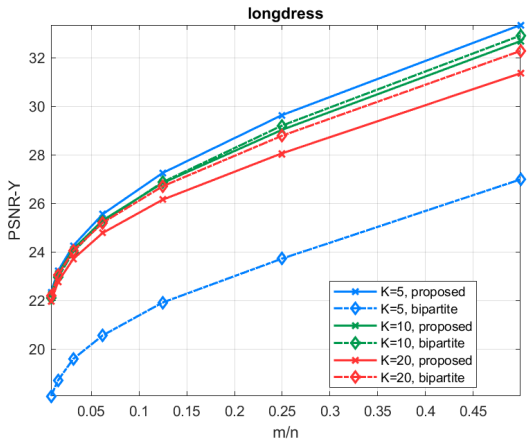

Fig. 2: Linear approximation of 3D point clouds attributes using iterated two channel filter-banks.

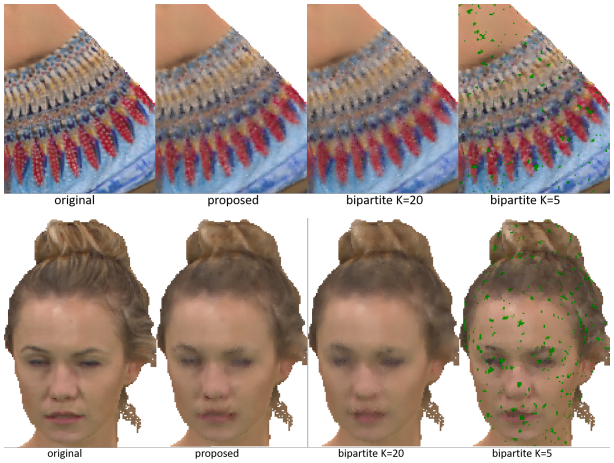

Fig. 3: Top $m/n = 0.25$, bottom $m/n = 0.125$. Comparison of linear approximation using BFB and proposed filter-banks.

5. NUMERICAL RESULTS

We implement a "lazy" bi-orthogonal filter-bank, with filters $\mathbf{H}_0 = \mathbf{I}$, $\mathbf{H}_1 = \mathbf{Z}$, $\mathbf{G}_0 = 2\mathbf{I} - \mathbf{Z}$, and $\mathbf{G}_1 = \mathbf{I}$. The down-sampling set $\mathcal{A}$ is chosen so that a node $i \in \mathcal{A}$ with probability $1/2$, leading to $|\mathcal{A}| \approx |\mathcal{B}|$. We iterate this filter-bank in the low pass channel L times, producing L high frequency channels, and 1 low pass channel. The low pass channel has approximately $n2^{-L}$ coefficients, while the ℓ-th level high pass channel has approximately $n2^{-\ell}$ coefficients.

3D point clouds consist of a list of points in 3D space represented by their coordinates $\mathbf{v}_i = [x_i, y_i, z_i]$, and attributes $\mathbf{a}_i$. We use the "longdress" point cloud from the "8iVFBv2" dataset [33], which comes with color attributes. Each point $\mathbf{v}_i$ is assigned a node in a graph, and an edge between nodes i and j is added if i is one of the K nearest neighbors of j, or vice versa. Edge weights are computed as $w_{ij} = 1/\|\mathbf{v}_i - \mathbf{v}_j\|$. Point cloud down-sampling corresponds to selecting a subset of points, therefore we can repeat this graph construction procedure on a smaller point cloud, at the output of the low pass channel. For each two-channel filter-bank we follow the steps: 1) construct a graph with K nearest neighbor (KNN) algorithm and compute its combinatorial Laplacian matrix, 2) generate a random down-sampling set $\mathcal{A}$, and $\mathcal{B} = \mathcal{A}^c$, and 3) if a bipartite graph is desired, keep edges between $\mathcal{A}$ and $\mathcal{B}$ and remove the rest.

Signal representation. We apply the iterated filter-bank with $L = 7$ levels to the color attributes of a single frame of the "longdress" sequence. For each L, we reconstruct the color signal using only the low frequency coefficients. We compare the proposed filter-banks with the BFBs as a function of m/n, where m is the number of coefficients in the low pass channel, and n is the total number of coefficients. Figure 2 shows that the proposed filter-bank has the best energy compaction when the KNN graph has fewer edges ($K = 5$), and performance decreases as K increases. The best performance of the BFBs is achieved with an intermediate value of $K = 10$. In Figure 3 we show the reconstructions of regions of the point cloud. When the bipartite graph is too sparse ($K = 5$), several artifacts can be observed, which can be attributed to points/nodes in the high pass channel that do not have connections in the low pass channel. When the bipartite graph is denser $K = 20$, the reconstruction has no artifacts, however details are smoothed more aggressively. The proposed filter-bank, with a sparser graph, better preserves textures and facial features (e.g., eyes, mouth and hair).

Complexity. We compare the run time of the iterated analysis filter-bank ($L = 7$) applied to 20 frames of the "longdress" sequence. We run the experiment using Matlab 2019. The bipartite filter-bank with $K = 20$ and $K = 10$ takes 14.3 and 8.23 seconds per frame respectively, while the proposed filter-bank with the best performance ($K = 5$), takes 6.72 seconds per frame. These point clouds have an average of $795,000$ points per frame. The complexity of our implementation is dominated by two factors. Graph construction, which is implemented using approximate KNN, with complexity proportional to K. Complexity of filtering is dominated by the product $\mathbf{Zx}$. When the graph is bipartite, $\mathbf{Zx}$ is a sparse matrix-vector product. In the non-bipartite case, $\mathbf{Zx}$ is computed in two steps, first we perform a sparse matrix-vector product $\mathbf{y} = \mathbf{Lx}$, and then solve the linear system $\mathbf{Qz} = \mathbf{y}$. Since $\mathbf{Q}$ is sparse, a numerically accurate approximation of $\mathbf{z} = \mathbf{Q}^{-1}\mathbf{y}$ can be found efficiently using the "\" operator in Matlab.

6. CONCLUSION

This paper extended the graph filter-bank framework of [5, 6], which uses the normalized Laplacian of bipartite graphs, to positive semi-definite variation operators, arbitrary graphs, and arbitrary down-sampling operators. We achieve this by proving that the spectral folding property is not unique to the normalized Laplacian of bipartite graphs, and in fact, it is satisfied by certain generalized eigenvalues and eigenvectors of non-bipartite graphs. Based on this, we proposed a new $\mathbf{Q}$-orthogonal graph Fourier transform, that leads to perfect reconstruction, orthogonal and bi-orthogonal conditions, equivalent to those already known for the bipartite graph case. We implemented a simple degree 1 polynomial "lazy" filter-bank on 3D point clouds graphs with hundreds of thousands of vertices (points). Our numerical results indicate that our framework outperforms the lazy filter-bank, implemented with bipartite graphs at various sparsity levels, in terms of run-time and energy compaction.

7. REFERENCES

[1] A. Ortega, P. Frossard, J. Kovačević, J.M.F. Moura, and P. Vandergheynst, "Graph signal processing: Overview, challenges, and applications," *Proceedings of the IEEE*, vol. 106, no. 5, pp. 808–828, 2018.

[2] D.I. Shuman, S.K. Narang, P. Frossard, A. Ortega, and P. Vandergheynst, "The emerging field of signal processing on graphs: Extending high-dimensional data analysis to networks and other irregular domains," *IEEE Signal Processing Magazine*, vol. 30, no. 3, pp. 83–98, 2013.

[3] Martin Vetterli and Jelena Kovacevic, *Wavelets and subband coding*, Prentice-hall, 1995.

[4] David I Shuman, "Localized spectral graph filter frames: A unifying framework, survey of design considerations, and numerical comparison," *IEEE Signal Processing Magazine*, vol. 37, no. 6, pp. 43–63, 2020.

[5] S.K. Narang and A. Ortega, "Perfect reconstruction two-channel wavelet filter banks for graph structured data," *IEEE Trans. on Signal Proc.*, vol. 60, no. 6, pp. 2786–2799, 2012.

[6] S.K. Narang and A. Ortega, "Compact support biorthogonal wavelet filterbanks for arbitrary undirected graphs," *IEEE Trans. on Signal Proc.*, vol. 61, no. 19, pp. 4673–4685, 2013.

[7] M.S. Kotzagiannidis and P.L. Dragotti, "Splines and wavelets on circulant graphs," *Applied and Computational Harmonic Analysis*, vol. 47, no. 2, pp. 481–515, 2019.

[8] A. Sakiyama, K. Watanabe, and Y. Tanaka, "Spectral graph wavelets and filter banks with low approximation error," *IEEE Trans. on Signal and Information Processing over Networks*, vol. 2, no. 3, pp. 230–245, 2016.

[9] D.B.H. Tay and J. Zhang, "Techniques for constructing biorthogonal bipartite graph filter banks," *IEEE Trans. on Signal Processing*, vol. 63, no. 21, pp. 5772–5783, 2015.

[10] D.B.H. Tay and A. Ortega, "Bipartite graph filter banks: Polyphase analysis and generalization," *IEEE Trans. on Signal Processing*, vol. 65, no. 18, pp. 4833–4846, 2017.

[11] A. Anis, P.A. Chou, and A. Ortega, "Compression of dynamic 3d point clouds using subdivisional meshes and graph wavelet transforms," in *2016 IEEE Intl. Conf. on Acoustics, Speech and Signal Processing (ICASSP)*. IEEE, 2016, pp. 6360–6364.

[12] D. E. O. Tzamarias, K. Chow, I. Blanes, and J. Serra-Sagristà, "Compression of hyperspectral scenes through integer-to-integer spectral graph transforms," *Remote Sensing*, vol. 11, no. 19, pp. 2290, 2019.

[13] M. Levorato, S. Narang, U. Mitra, and A. Ortega, "Reduced dimension policy iteration for wireless network control via multiscale analysis," in *2012 IEEE Global Communications Conference (GLOBECOM)*. IEEE, 2012, pp. 3886–3892.

[14] Y-L Qiao, Y. Zhao, and X-Y Men, "Target recognition in sar images via graph wavelet transform and 2dpca," in *Proceedings of the 2nd International Conference on Image and Graphics Processing*, 2019, pp. 3–7.

[15] B. Girault, A. Ortega, and S.S. Narayanan, "Irregularity-aware graph fourier transforms," *IEEE Transactions on Signal Processing*, vol. 66, no. 21, pp. 5746–5761, 2018.

[16] A. Anis, A. Gadde, and A. Ortega, "Efficient sampling set selection for bandlimited graph signals using graph spectral proxies," *IEEE Trans. on Signal Processing*, vol. 64, no. 14, pp. 3775–3789, 2016.

[17] H.E. Egilmez, E. Pavez, and A. Ortega, "Graph learning from data under laplacian and structural constraints," *IEEE J. of Selected Topics in Signal Proc.*, vol. 11, no. 6, pp. 825–841, 2017.

[18] E. Pavez, B. Girault, A. Ortega, and Philip A. Chou, "Region adaptive graph Fourier transform for 3D point clouds," in *International Conference on Image Processing (ICIP)*, 2020.

[19] B. Girault, A. Ortega, and S. S. Narayayan, "Graph vertex sampling with arbitrary graph signal hilbert spaces," in *2020 IEEE International Conference on Acoustics, Speech and Signal Processing (ICASSP)*. IEEE, 2020, pp. 5670–5674.

[20] Fan RK Chung, *Spectral graph theory*, Number 92. American Mathematical Soc., 1997.

[21] M. Crovella and E. Kolaczyk, "Graph wavelets for spatial traffic analysis," in *IEEE INFOCOM 2003. Twenty-second Annual Joint Conference of the IEEE Computer and Communications Societies*. IEEE, 2003, vol. 3, pp. 1848–1857.

[22] R.R. Coifman and M. Maggioni, "Diffusion wavelets," *Applied and Computational Harmonic Analysis*, vol. 21, no. 1, pp. 53–94, 2006.

[23] D.K. Hammond, P. Vandergheynst, and R. Gribonval, "Wavelets on graphs via spectral graph theory," *Applied and Computational Harmonic Analysis*, vol. 30, no. 2, pp. 129–150, 2011.

[24] D. I. Shuman, M. J. Faraji, and P. Vandergheynst, "A multiscale pyramid transform for graph signals," *IEEE Trans. on Signal Processing*, vol. 64, no. 8, pp. 2119–2134, 2015.

[25] A. Sakiyama and Y. Tanaka, "Oversampled graph laplacian matrix for graph filter banks," *IEEE Trans. on Signal Processing*, vol. 62, no. 24, pp. 6425–6437, 2014.

[26] S. Li, Y. Jin, and D. I. Shuman, "Scalable m-channel critically sampled filter banks for graph signals," *IEEE Trans. on Signal Processing*, vol. 67, no. 15, pp. 3954–3969, 2019.

[27] A. Anis and A. Ortega, "Critical sampling for wavelet filterbanks on arbitrary graphs," in *2017 IEEE Intl. Conf. on Acoustics, Speech and Signal Processing (ICASSP)*. IEEE, 2017, pp. 3889–3893.

[28] S.K. Narang and A. Ortega, "Local two-channel critically sampled filter-banks on graphs," in *2010 IEEE International Conf. on Image Processing*. IEEE, 2010, pp. 333–336.

[29] J. Zeng, G. Cheung, and A. Ortega, "Bipartite approximation for graph wavelet signal decomposition," *IEEE Transactions on Signal Processing*, vol. 65, no. 20, pp. 5466–5480, 2017.

[30] A. Jiang, J. Wan, Y. Tang, B. Ni, and Y. Zhu, "Admm-based bipartite graph approximation," in *ICASSP 2019-2019 IEEE Intl. Conf. on Acoustics, Speech and Signal Processing (ICASSP)*. IEEE, 2019, pp. 5421–5425.

[31] A. Sakiyama, K. Watanabe, Y. Tanaka, and A. Ortega, "Two-channel critically sampled graph filter banks with spectral domain sampling," *IEEE Trans. on Signal Processing*, vol. 67, no. 6, pp. 1447–1460, 2019.

[32] E. Pavez, B. Girault, A. Ortega, and P. A. Chou, "Two channel filterbanks on arbitrary graphs with positive semidefinite variation operators," *arXiv preprint*, 2021.

[33] E. d'Eon, B. Harrison, T. Myers, and P. A. Chou, "8i voxelized full bodies-a voxelized point cloud dataset," *ISO/IEC JTC1/SC29 Joint WG11/WG1 (MPEG/JPEG) input document WG11M40059/WG1M74006*, 2017.